

A Calix[4]resorcinarene-Based [Co₁₂] Coordination Cage for Highly Efficient Cycloaddition of CO₂ to Epoxides

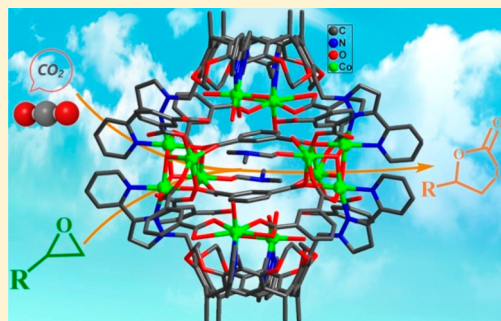
Ting-Ting Guo,^{†,§} Xiao-Fang Su,^{†,§} Xianxiu Xu,[‡] Jin Yang,^{*,†} Li-Kai Yan,^{†,ie} and Jian-Fang Ma^{*,†,ie}

[†]Key Lab for Polyoxometalate Science, Department of Chemistry, Northeast Normal University, Changchun 130024, China

[‡]College of Chemistry, Chemical Engineering and Materials Science, Key Laboratory of Molecular and Nano Probes, Ministry of Education, Shandong Normal University, Jinan 250014, China

Supporting Information

ABSTRACT: The design and synthesis of polynuclear metal cluster-based coordination cages is of considerable interest due to their appealing structural characteristics and potential applications. Herein, we report a calix[4]resorcinarene-based [Co₁₂] coordination cage, [Co₁₂(TPC4R-I)₂(1,3-BDC)₁₀(μ₃-OH)₄(H₂O)₁₀(DMF)₂·7DMF·23H₂O (**1**), assembled with 2 bowl-shaped calix[4]resorcinarenes (TPC4R-I), 10 angular 1,3-benzenedicarboxylates (1,3-BDC), and 12 Co(II) cations. Remarkably, it is shown to be a highly efficient recyclable heterogeneous catalyst for CO₂ conversion due to its exposed Co(II) Lewis acid sites.



INTRODUCTION

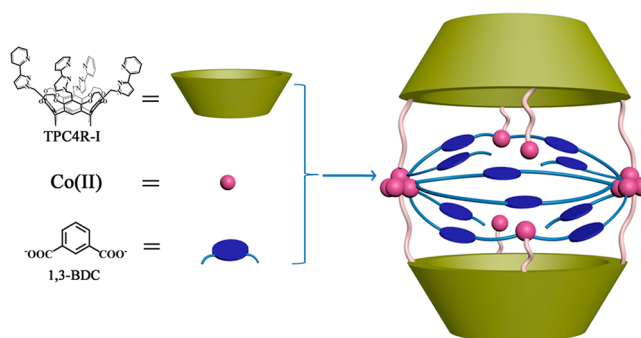
The design and assembly of polynuclear metal cluster-based coordination cages have attracted great interest due to their unique structures and broad applications including gas sorption, drug delivery, and catalysis.^{1–11} Notably, organic linkers with special structural features play a key role in controlling structures of the polynuclear metal cluster-based coordination cages.^{12–14} In this context, calix[4]arenes have been widely used in coordination chemistry.^{15–21} Among them, calix[4]resorcinarenes are exceedingly attractive supramolecules owing to their special structural features modified by functionalized groups.^{22–27} As a result, the design and assembly of the polynuclear metal cluster-based coordination cages with calix[4]resorcinarenes are quite desirable yet remain a synthetic challenge.²⁸

Carbon dioxide (CO₂) is responsible for the increasing global warming as well as exacerbating climate changes as a major greenhouse gas.²⁹ The chemical conversion of CO₂ via the catalytic reaction is an attractive method for the recycling of carbons.^{30–32} In this regard, the CO₂ cycloaddition to epoxides has attracted considerable attention.³³ To date, numerous catalysts have been developed for the cycloaddition of CO₂ with epoxides.^{34–36} The polynuclear metal cluster-based coordination cages with metal Lewis acid sites, as an emerging type of heterogeneous catalysts, have received increasing interest owing to their easy separation and reuse in catalysis.^{36,37} However, nearly no polynuclear metal cluster-based coordination cages with calix[4]resorcinarenes have been applied as heterogeneous catalysts for the CO₂ cycloaddition to epoxides thus far.³⁷

Based on the considerations above, an appropriate angular 1,3-benzenedicarboxylic acid (1,3-H₂BDC) was used to tune

the assembly of calix[4]resorcinarene-based (TPC4R-I) coordination cage. Herein, a remarkable [Co₁₂] coordination cage with [Co₄O₄] cubanes, namely, [Co₁₂(TPC4R-I)₂(1,3-BDC)₁₀(μ₃-OH)₄(H₂O)₁₀(DMF)₂·7DMF·23H₂O (**1**), was assembled with functionalized calix[4]resorcinarene (TPC4R-I), angular 1,3-H₂BDC, and Co(II) cations (Scheme 1). Notably, **1** represents a unique example of [Co₁₂] coordination cages with [Co₄O₄] cubanes surrounded by calix[4]resorcinarenes. Importantly, **1** features highly efficient cycloaddition of CO₂ with epoxides as a recyclable heterogeneous catalyst.

Scheme 1. Construction of Calix[4]resorcinarene-Based [Co₁₂] Cage of **1**^a



^aThe coordinated water and DMF molecules are not shown for clarity.

Received: August 14, 2019

RESULTS AND DISCUSSION

Crystal Structure of 1. The formula of **1** is established by X-ray diffraction analysis, thermogravimetric analysis, as well as elemental analysis. Crystallographic diffraction demonstrates that **1** features an unusual calix[4]resorcinarene-based [Co₁₂] coordination cage assembled with two independent [Co₄O₄] cubanes and four independent mononuclear Co(II) cations (Figure 1). Two pairs of centrosymmetrically related [Co₄O₄]

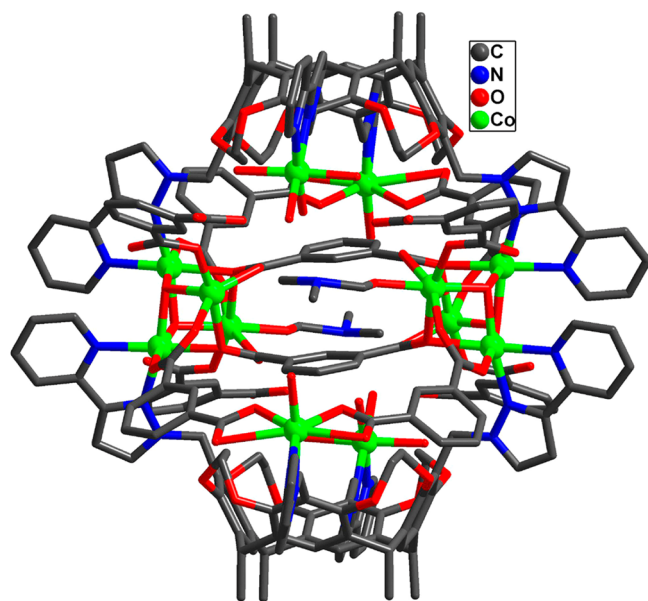


Figure 1. Crystal structure of [Co₁₂] coordination cage of **1**.

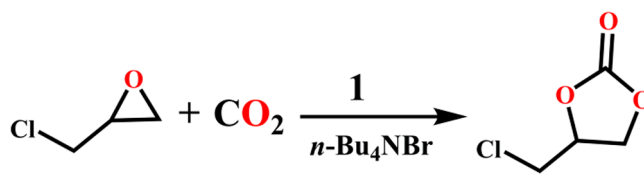
cubanes and four mononuclear Co(II) cations are bridged by the 1,3-BDC anions to produce the remarkable [Co₁₂] coordination cage, which is further ligated by two TPC4R-I species on both sides (Figure 1). The [Co₄O₄] cubane consists of four Co(II) cations, two *u*₂-O atoms, and two *u*₃-O atoms (Figure S1a). Each Co(II) cation in the [Co₄O₄] cubane is linked by the *u*₂-O and *u*₃-O atoms. Notably, two 2-(pyrazol-3-yl)pyridine groups from two different TPC4R-I species chelate two Co(II) cations of one [Co₄O₄] cubane, thus highly stabilizing the [Co₄O₄] cubane. The Co–O distances in the [Co₄O₄] cubane range from 2.006(4) to 2.325(4) Å, and the Co···Co separations by the oxygen atoms vary from 3.09 to 3.66 Å. To our knowledge, **1** represents a unique example of [Co₁₂] coordination cages with [Co₄O₄] cubanes surrounded by calix[4]resorcinarenes. Bond valence sum (BVS) calculations indicate that the cobalt atoms are in +2 oxidation state (Table S1). After removal of solvents, the free void volume in each unit cell is about 39.7% according to calculation with PLATON.³⁸

Notably, we recently reported two related [Co₁₆] cages, [Co₁₆(TPC4R-I)₂(HL)₄(L)₈(H₂O)₂₄]·12DMF·4H₂O (**1-SO₃H**) and [Co₁₆(TPC4R-I)₂(HL1)₄(L1)₈(H₂O)₁₆]·17DMA·H₂O (**1-OH**) (H₃L = 5-sulfonic-isophthalic acid, H₃L1 = 5-hydroxy-isophthalic acid, and DMA = *N,N'*-dimethylacetamide).²² Each [Co₁₆] cage consists of 16 Co(II) cations, 2 calix[4]resorcinarenes, and 12 angular isophthalate derivatives. Obviously, the two types of [Co₁₂] and [Co₁₆] cages were prepared from the analogous precursors under similar reaction conditions (e.g., reaction temperatures and solvents), but their cage structures are completely different.

Based on our experiments and the cage structures, we can infer that the substituents (–SO₃H and –OH vs –H) of the isophthalate derivatives play a key role in the construction of different cage motifs. In other words, the formation of the [Co₁₂] and [Co₁₆] cages is highly dependent on the additional negative charges of the isophthalate derivatives used.²²

Cycloaddition of CO₂ with Epoxides. Given the Co(II) Lewis acid sites in **1**, the CO₂ cycloaddition to epoxide was studied in detail.^{39–41} Prior to the catalytic study, **1** was activated to remove the coordinated water and DMF molecules.^{42,43} Typically, **1** was solvent-exchanged with dry acetone for at least ten times over 3 days. Then, the sample was filtered and activated at 80 °C under vacuum for more than 10 h. Initially, the cycloaddition between epichlorohydrin (ECH) and CO₂ was utilized as the model to scout for the optimum reaction conditions (Scheme 2). After the catalytic reactions

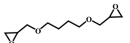
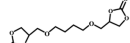
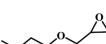
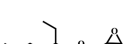
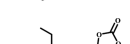
Scheme 2. Schematic Drawing for Cycloaddition of CO₂ with ECH



finished, the reaction flask was immediately placed in cold water. Then, the residue was washed with cold CH₂Cl₂ (3 mL) and centrifuged to isolate the products. The reaction products were then purified by extraction with a mixture of CH₂Cl₂ and water (8 mL, 1/1 v/v). The product carbonates were characterized by ¹H NMR (Figures S2–S10). The corresponding conversions were determined by gas chromatography (GC) (Figures S11 and S12). As listed in Table S2, the CO₂ cycloaddition with ECH by **1** (0.002 mmol) gave only 25% conversion after 6 h in the absence of tetra-*n*-butylammonium bromide (*n*-Bu₄NBr). Accordingly, a conversion of ca. 47% was achieved with only *n*-Bu₄NBr as catalyst under the same reaction condition (entry 2, Table S2). Notably, when *n*-Bu₄NBr and **1** were applied as cocatalysts, the conversion of ECH was significantly enhanced to 96% (entry 4, Table S2). Moreover, the conversion of ECH was investigated with different amounts of **1** under the same condition. When the amount of **1** reached 0.003 mmol, the conversion was enhanced to 98% after 6 h (entries 3–5, Table S2). Further, under elevated reaction temperatures from 30 to 60 °C, the corresponding conversions of ECH increased from 30% to the final 96% after 6 h (entries 4 and 6–8, Table S2). Noticeably, compared to the activated sample of **1**, the unactivated one gave the relatively low conversion (entry 9, Table S2). As a result, subsequent studies on cycloadditions of CO₂ with epoxides were carried out with *n*-Bu₄NBr (0.25 mmol) and the activated sample of **1** (0.002 mmol) at 60 °C and 1 atm CO₂ for 6 h.

To explore the applicability of the catalytic reactions, the epoxides with different structures were studied as substrates.^{44–48} The cycloaddition of CO₂ with ECH, 1,4-bis(oxiran-2-ylmethoxy)butane (BOMB), 2-((benzyloxy)methyl)oxirane (BMO), 2-(phenoxymethyl)oxirane (PMO), and 2-(butoxymethyl)oxirane (2-BMO) (entries 1–5, Table 1) afford the high conversions of 96%, 96%, 86%, 86%, and 81%, respectively, within 6 h. In contrast, when the electron-donors

Table 1. Cycloaddition of CO₂ with Different Epoxides by **1**^a

Entry	Epoxide	Product	Time (h)	Conversion (%)	Time (h)	Conversion (%)
1			6	96	12	99
2			6	96	12	99
3			6	86	12	99
4			6	86	12	99
5			6	81	12	99
6			6	79	12	92
7			6	75	12	98
8			6	40	12	82
9			6	61	12	83

^aReaction conditions: **1** (0.002 mmol), *n*-Bu₄NBr (0.25 mmol), epoxide (5 mmol), CO₂ (1 atm), and 60 °C.

1,4-di(oxiran-2-yl)butane (DOB), 2-butyloxirane (2-BO), and 2-phenyloxirane (2-PO) were utilized as substrates, the corresponding conversions were reduced (entries 6–8, Table 1). However, only 61% of the overall 2-(((2-ethylhexyl)oxy)methyl)oxirane (EOMO) was converted into the product under the same condition (entry 9, Table 1), which can be attributed to the high steric hindrance of substrate.^{49–51} Further, when the reaction time reached 12 h, most of the substrates were completely converted into the catalytic products (entries 1–7, Table 1). In contrast, the conversions of the electron-donor 2-PO and the steric hindrance EOMO were only 82% and 83%, respectively, after 12 h (entries 8 and 9). Noticeably, within 12 h, the epoxide was converted into the single cyclic carbonate with >99% selectivity determined by ¹H NMR data (Table S3).⁵²

Moreover, catalytic kinetics for the cycloaddition of PMO with CO₂ was also studied with **1** and *n*-Bu₄NBr as cocatalysts. The catalytic experiment was conducted at different reaction time intervals. With the increasing reaction time, the conversions of the substrate PMO were gradually enhanced, as depicted in Figure 2a. After 6 h, ca. 86% of PMO was converted into the target product, and the final conversion reached 97% after 8 h.

Notably, **1** can be recovered from the reaction system by centrifugation, washed with acetone, and dried under vacuum at 50 °C before the next catalytic cycle. As illustrated in Figure 2b, **1** still retains the high catalytic performance after five runs, demonstrating its good reusability during the CO₂ cycloaddition with epoxides. In addition, the heterogeneity was also studied for the catalytic reaction. **1** was removed after 4 h of the catalytic reaction. As depicted in Figure 2a, no obvious increase was observed for the catalytic product in the filtrate, suggesting the heterogeneity of the catalysis. The PXRD

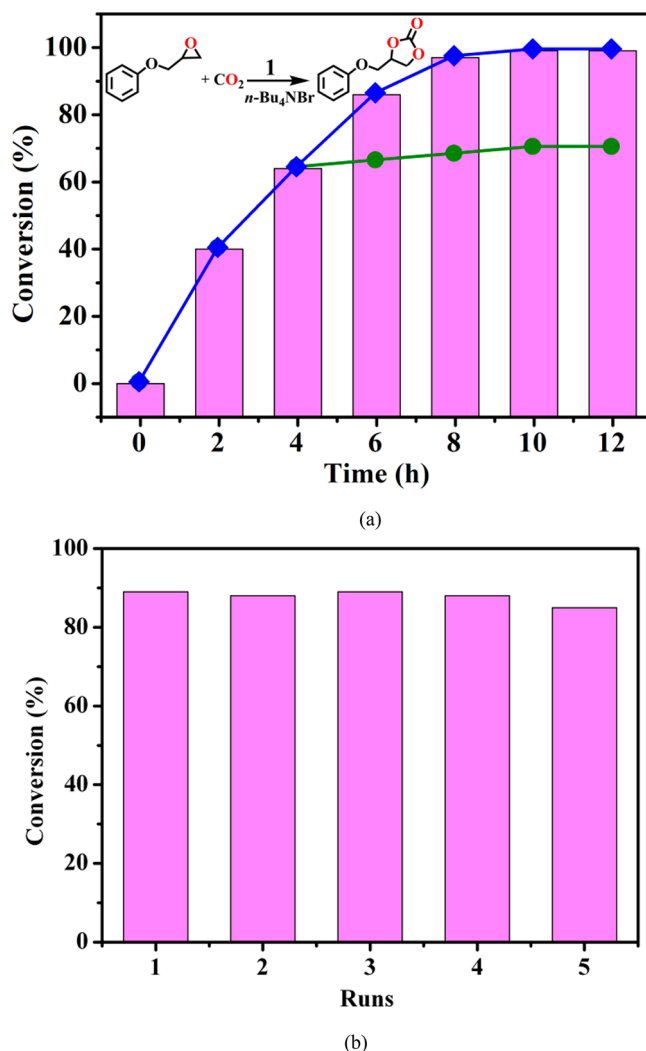


Figure 2. (a) Catalytic dynamic study for the cycloaddition of CO₂ with PMO catalyzed by **1** (blue) and filtrate (green). (b) Recyclable cycloaddition of CO₂ with PMO using **1** as catalyst.

pattern of **1** after the cycloaddition reaction was determined and demonstrated its structural integrity after catalysis (Figure S13a). Overall, the high catalytic activity and easy reusability made **1** an excellent catalyst for CO₂ cycloaddition to epoxides.

Additionally, **1** features the high catalytic efficiency for the cycloaddition of CO₂ under relatively mild conditions. The catalytic activities of **1** toward the CO₂ cycloaddition reactions are comparable to the known metal organic compounds (Table S4). For example, for the reaction time of 6 h, the conversion of ECH for **1** is 96% at 60 °C and 1 atm CO₂, while the corresponding conversion for catalyst [Zr₆(μ₃-OH)₈(OH)₈(Cu-L2)₄] (L2 = 6,13-dicarboxy-1,4,8,11-tetraazacyclotetradecane) (a) reached 94% at increased temperature (90 °C) and gas pressure (10 atm) (Table S4).⁵³ For PMO, the 64% conversion was achieved with **1** as catalyst at 60 °C for 4 h, whereas the conversion is only 41% for catalyst {[Mn₃(L3)(H₂O)₆(DMA)₂]·5DMA·4C₂H₅OH} (L3 = 5,10,15,20-tetra(4-(3,5-dicarboxylphenoxy)phenyl)porphyrin) (b) at 80 °C for 4 h.⁴⁹ Notably, the substrate PMO was completely converted with **1** as catalyst at 60 °C for 12 h. Nevertheless, the similar conversions of PMO were acquired when the reaction temperatures were elevated to 80 and 100 °C for {[(CH₃)₂NH₂]₆[Cd₃(L4)(H₂O)₂]}·12H₂O (L4 =

resorcin[4]arene-functionalized dodecarboxylate) (c) and $[\text{Ni}_2(\text{L5})(\text{DMF})(\text{H}_2\text{O})_4]$ (L5 = tetrakis(4-carboxyphenyl)-ethylene) (d), respectively (Table S4).^{37,42} These results demonstrate that the catalytic performance of **1** is comparable to those of the metal organic compounds determined at high reaction temperatures and elevated gas pressures.

Moreover, the catalytic activity of **1** for the CO_2 cycloaddition is comparable to the related mononuclear, dinuclear, or tetranuclear metal cation-based complexes (Table S5). For instance, an 82% conversion of 2-PO was acquired using **1** as catalyst at 60 °C for 12 h, while the similar conversion was achieved even at increased reaction temperature (100 °C) for mononuclear Co(II)-based $\{[\text{Co}(\text{L6})(\text{L7})(2\text{H}_2\text{O})]\cdot 2\text{H}_2\text{O}\}_n$ (L6 = *trans,trans*-muconate dianion and L7 1,2-bis(4-pyridyl)-ethane) (e).⁵⁴ Particularly, the same conversion was obtained for dinuclear Co(II)-based $\{[\text{Co}_6(\text{L8})_4(\text{L9})_3(\text{H}_2\text{O})_3]\cdot 12\text{DMF}\cdot 9\text{H}_2\text{O}\}_n$ (f) (L8 = 4,4',4''-s-triazine-1,3,5-triyl-tri-*p*-aminobenzate and L9 = 1,4-diazabicyclo[2.2.2]octane), when the reaction temperature was elevated to 80 °C and the reaction time was prolonged to 15 h (Table S5).⁵⁵ Noticeably, the final conversion of 2-PO is only 68% for tetranuclear Ni(II)-based $\{[\text{Ni}_4(\text{L10})(\mu_3\text{-OH})_2(\text{H}_2\text{O})_6]\cdot 2\text{H}_2\text{O}\cdot \text{DMA}\}_n$ (L10 = 5,5',5''-(methylsilanetriyl)trisophthalate) (g) at increased reaction temperature (100 °C) and gas pressure (10 atm).⁵⁶

It is well-established that the metal cation Lewis acids could act as the catalytic active sites for the CO_2 cycloaddition reactions.^{57–62} The coordinated water molecules and solvents in the single Co(II) cation and the $[\text{Co}_4\text{O}_4]$ unit were removed by fully activating the sample of **1** before the catalytic study. Thereby, the single Co(II) cation and the $[\text{Co}_4\text{O}_4]$ unit in **1** feature the exposed Lewis acid sites and act as the catalytic centers, which resulted in a synergistic effect for the cycloaddition reaction of CO_2 .

To further explore the role of the whole cage structure in the CO_2 cycloaddition reaction, the reference experiment for the cycloaddition of ECH and CO_2 was conducted using cobalt acetate (0.002 mmol) and *n*-Bu₄NBr (0.25 mmol) under the same condition.⁵⁴ A total conversion of 67% was obtained with cobalt acetate and *n*-Bu₄NBr as cocatalysts at 60 °C for 6 h (Table S2). Obviously, this conversion is much lower than that (96%) with **1** and *n*-Bu₄NBr as cocatalysts. The result suggests that the whole cage structure with rich Lewis acid Co(II) sites is effective for improving the CO_2 cycloaddition to epoxides. In addition, the ICP analysis of the filtrate after the cycloaddition of CO_2 ruled out the leaching of the Co(II) cations from **1**, confirming the whole cage as the catalyst.

CONCLUSIONS

In summary, we present a calix[4]resorcinarene-based $[\text{Co}_{12}]$ coordination cage **1**, constructed by 2 bowl-shaped calix[4]-resorcinarenes, 10 angular 1,3-benzenedicarboxylates, and 12 Co(II) cations. **1** represents an unusual example of $[\text{Co}_{12}]$ coordination cages with $[\text{Co}_4\text{O}_4]$ cubanes surrounded by calix[4]resorcinarenes. Importantly, the activated sample of **1** with exposed Lewis acidic sites, as a recyclable catalyst, features high catalytic activities for CO_2 cycloaddition to epoxides. This work offers a feasible route for the design and synthesis of functional polynuclear metal cluster-based coordination cages. Further efforts to assemble the calix[4]resorcinarene-based cages featuring elegant motifs and potential applications are ongoing in our lab.

ASSOCIATED CONTENT

Supporting Information

The Supporting Information is available free of charge at <https://pubs.acs.org/doi/10.1021/acs.inorgchem.9b02473>.

Experimental section, crystallographic data, ¹H NMR spectra, tables of data, and GC spectra (PDF)

Accession Codes

CCDC 1941476 contains the supplementary crystallographic data for this paper. These data can be obtained free of charge via www.ccdc.cam.ac.uk/data_request/cif, or by emailing data_request@ccdc.cam.ac.uk, or by contacting The Cambridge Crystallographic Data Centre, 12 Union Road, Cambridge CB2 1EZ, UK; fax: +44 1223 336033.

AUTHOR INFORMATION

Corresponding Authors

*E-mail: yangj808@nenu.edu.cn. (J.Y.)

*E-mail: majf247@nenu.edu.cn. Fax: +86-431-85098620. (J.-F.M.)

ORCID

Li-Kai Yan: 0000-0002-1352-4095

Jian-Fang Ma: 0000-0002-4059-8348

Author Contributions

[§]T.-T.G. and X.-F.S. contributed equally to this manuscript.

Notes

The authors declare no competing financial interest.

ACKNOWLEDGMENTS

This work was supported by the National Natural Science Foundation of China (21771034 and 21471029).

REFERENCES

- (1) Cook, T. R.; Stang, P. J. Recent Developments in the Preparation and Chemistry of Metallacycles and Metallacages via Coordination. *Chem. Rev.* **2015**, *115*, 7001–7045.
- (2) Brown, C. J.; Toste, F. D.; Bergman, R. G.; Raymond, K. N. Supramolecular Catalysis in Metal–Ligand Cluster Hosts. *Chem. Rev.* **2015**, *115*, 3012–3035.
- (3) Zhang, G.; Mastalerz, M. Organic Cage Compounds—from Shape-Persistency to Function. *Chem. Soc. Rev.* **2014**, *43*, 1934–1947.
- (4) Geng, D.; Han, X.; Bi, Y.; Qin, Y.; Li, Q.; Huang, L.; Zhou, K.; Song, L.; Zheng, Z. Merohedra Icosahedral M₄₈ (M = Co^{II}, Ni^{II}) Cage Clusters Supported by Thiacalix[4]arene. *Chem. Sci.* **2018**, *9*, 8535–8541.
- (5) Bi, Y.; Du, S.; Liao, W. Thiacalixarene-Based Nanoscale Polyhedral Coordination Cages. *Coord. Chem. Rev.* **2014**, *276*, 61–72.
- (6) Jin, P.; Dalgarno, S. J.; Atwood, J. L. Mixed Metal–Organic Nanocapsules. *Coord. Chem. Rev.* **2010**, *254*, 1760–1768.
- (7) Dalton, D. M.; Ellis, S. R.; Nichols, E. M.; Mathies, R. A.; Toste, F. D.; Bergman, R. G.; Raymond, K. N. Supramolecular Ga₄L₆¹²⁻ Cage Photosensitizes 1,3-Rearrangement of Encapsulated Guest via Photoinduced Electron Transfer. *J. Am. Chem. Soc.* **2015**, *137*, 10128–10131.
- (8) Mondal, B.; Mukherjee, P. S. Cage Encapsulated Gold Nanoparticles as Heterogeneous Photocatalyst for Facile and Selective Reduction of Nitroarenes to Azo Compounds. *J. Am. Chem. Soc.* **2018**, *140*, 12592–12601.
- (9) Liu, M.; Liao, W.; Hu, C.; Du, S.; Zhang, H. Calixarene-Based Nanoscale Coordination Cages. *Angew. Chem., Int. Ed.* **2012**, *51*, 1585–1588.
- (10) Wang, S.; Sawada, T.; Ohara, K.; Yamaguchi, K.; Fujita, M. Capsule–Capsule Conversion by Guest Encapsulation. *Angew. Chem., Int. Ed.* **2016**, *55*, 2063–2066.

- (11) Rizzuto, F. J.; Ramsay, W. J.; Nitschke, J. R. Otherwise Unstable Structures Self-Assemble in the Cavities of Cuboctahedral Coordination Cages. *J. Am. Chem. Soc.* **2018**, *140*, 11502–11509.
- (12) Rathnayake, A. S.; Fraser, H. W. L.; Brechin, E. K.; Dalgarno, S. J.; Baumeister, J. E.; Rungthanaphatsophon, P.; Walensky, J. R.; Barnes, C. L.; Atwood, J. L. Oxidation State Distributions Provide Insight into Parameters Directing the Assembly of Metal–Organic Nanocapsules. *J. Am. Chem. Soc.* **2018**, *140*, 13022–13027.
- (13) Mastalerz, M. Shape-Persistent Organic Cage Compounds by Dynamic Covalent Bond Formation. *Angew. Chem., Int. Ed.* **2010**, *49*, 5042–5053.
- (14) Acharyya, K.; Mukherjee, P. S. Organic Imine Cages: Molecular Marriage and Applications. *Angew. Chem., Int. Ed.* **2019**, *58*, 8640–8653.
- (15) Joseph, R.; Rao, C. P. Ion and Molecular Recognition by Lower Rim 1,3-Di-conjugates of Calix[4]arene as Receptors. *Chem. Rev.* **2011**, *111*, 4658–4702.
- (16) Mattiuzzi, A.; Jabin, I.; Mangeney, C.; Roux, C.; Reinaud, O.; Santos, L.; Bergamini, J.-F.; Hapiot, P.; Lagrost, C. Electrografting of Calix[4]arene Diazonium Salts to Form Versatile Robust Platforms for Spatially Controlled Surface Functionalization. *Nat. Commun.* **2012**, *3*, 1130.
- (17) Wang, S.; Gao, X.; Hang, X.; Zhu, X.; Han, H.; Li, X.; Liao, W.; Chen, W. Calixarene-Based $\{Ni_{18}\}$ Coordination Wheel: Highly Efficient Electrocatalyst for the Glucose Oxidation and Template for the Homogenous Cluster Fabrication. *J. Am. Chem. Soc.* **2018**, *140*, 6271–6277.
- (18) Wang, S.; Gao, X.; Hang, X.; Zhu, X.; Han, H.; Liao, W.; Chen, W. Ultrafine Pt Nanoclusters Confined in a Calixarene-Based $\{Ni_{24}\}$ Coordination Cage for High-Efficient Hydrogen Evolution Reaction. *J. Am. Chem. Soc.* **2016**, *138*, 16236–16239.
- (19) Adhikari, L.; Larm, N. E.; Wagle, D. V.; Atwood, J. L.; Baker, G. A. Facile, One-Pot, in Aqua Synthesis of Catalytically Competent Gold Nanoparticles Using Pyrogallol[4]arene as The Sole Reagent. *Chem. Commun.* **2019**, *55*, 6261–6264.
- (20) Ling, I.; Kumari, H.; Mirzamani, M.; Sobolev, A. N.; Garvey, C. J.; Atwood, J. L.; Raston, C. L. Phase Dependent Structural Perturbation of a Robust Multicomponent Assembled Icosahedral Array. *Chem. Commun.* **2018**, *54*, 10824–10827.
- (21) Fang, Y.; Xiao, Z.; Li, J.; Lollar, C.; Liu, L.; Lian, X.; Yuan, S.; Banerjee, S.; Zhang, P.; Zhou, H.-C. Formation of a Highly Reactive Cobalt Nanocluster Crystal within a Highly Negatively Charged Porous Coordination Cage. *Angew. Chem., Int. Ed.* **2018**, *57*, 5283–5287.
- (22) Guo, T.-T.; Cheng, D.-M.; Yang, J.; Xu, X.; Ma, J.-F. Calix[4]resorcinarene-Based $[Co_{16}]$ Coordination Cages Mediated by Isomorphous Auxiliary Ligands for Enhanced Proton Conduction. *Chem. Commun.* **2019**, *55*, 6277–6280.
- (23) Kobayashi, K.; Yamanaka, M. Self-Assembled Capsules Based on Tetrafunctionalized Calix[4]resorcinarene Cavitands. *Chem. Soc. Rev.* **2015**, *44*, 449–466.
- (24) Kane, C. M.; Banisafar, A.; Dougherty, T. P.; Barbour, L. J.; Holman, K. T. Enclathration and Confinement of Small Gases by the Intrinsically 0D Porous Molecular Solid, Me₂H₂SiMe₂. *J. Am. Chem. Soc.* **2016**, *138*, 4377–4392.
- (25) Han, X.; Xu, Y.-X.; Yang, J.; Xu, X.; Li, C.-P.; Ma, J.-F. Metal-Assembled, Resorcin[4]arene-Based Molecular Trimer for Efficient Removal of Toxic Dichromate Pollutants and Knoevenagel Condensation Reaction. *ACS Appl. Mater. Interfaces* **2019**, *11*, 15591–15597.
- (26) Lu, B.-B.; Yang, J.; Che, G.-B.; Pei, W.-Y.; Ma, J.-F. Highly Stable Copper(I)-Based Metal–Organic Framework Assembled with Resorcin[4]arene and Polyoxometalate for Efficient Heterogeneous Catalysis of Azide–Alkyne “Click” Reaction. *ACS Appl. Mater. Interfaces* **2018**, *10*, 2628–2636.
- (27) Lv, L.-L.; Yang, J.; Zhang, H.-M.; Liu, Y.-Y.; Ma, J.-F. Metal-Ion Exchange, Small-Molecule Sensing, Selective Dye Adsorption, and Reversible Iodine Uptake of Three Coordination Polymers Constructed by a New Resorcin[4]arene-Based Tetracarboxylate. *Inorg. Chem.* **2015**, *54*, 1744–1755.
- (28) Pei, W.-Y.; Xu, G. H.; Yang, J.; Wu, H.; Chen, B. L.; Zhou, W.; Ma, J.-F. Versatile Assembly of Metal-Coordinated Calix[4]-resorcinarene Cavitands and Cages through Ancillary Linker Tuning. *J. Am. Chem. Soc.* **2017**, *139*, 7648–7656.
- (29) Tu, W.; Zhou, Y.; Zou, Z. Photocatalytic Conversion of CO₂ into Renewable Hydrocarbon Fuels: State-of-the-Art Accomplishment, Challenges, and Prospects. *Adv. Mater.* **2014**, *26*, 4607–4626.
- (30) Fu, Y.; Sun, D.; Chen, Y.; Huang, R.; Ding, Z.; Fu, X.; Li, Z. An Amine-Functionalized Titanium Metal–Organic Framework Photocatalyst with Visible-Light-Induced Activity for CO₂ Reduction. *Angew. Chem., Int. Ed.* **2012**, *51*, 3364–3367.
- (31) Huff, C. A.; Sanford, M. S. Cascade Catalysis for the Homogeneous Hydrogenation of CO₂ to Methanol. *J. Am. Chem. Soc.* **2011**, *133*, 18122–18125.
- (32) Chen, L.; Yu, F.; Shen, X.; Duan, C. N-CND Modified NH₂-UiO-66 for Photocatalytic CO₂ Conversion under Visible Light by a Photo-Induced Electron Transfer Process. *Chem. Commun.* **2019**, *55*, 4845–4848.
- (33) Yang, Q.; Yang, C.-C.; Lin, C.-H.; Jiang, H.-L. Metal–Organic Framework-Derived Hollow N-Doped Porous Carbon with Ultrahigh Concentrations of Single Zn Atoms for Efficient Carbon Dioxide Conversion. *Angew. Chem., Int. Ed.* **2019**, *58*, 3511–3515.
- (34) Bobbink, F. D.; Vasilyev, D.; Hulla, M.; Chamam, S.; Menoud, F.; Laurenczy, G.; Katsyuba, S.; Dyson, P. J. Intricacies of Cation–Anion Combinations in Imidazolium Salt Catalyzed Cycloaddition of CO₂ Into Epoxides. *ACS Catal.* **2018**, *8*, 2589–2594.
- (35) Li, P.-Z.; Wang, X.-J.; Liu, J.; Lim, J. S.; Zou, R.; Zhao, Y. A Triazole-Containing Metal–Organic Framework as a Highly Effective and Substrate Size-Dependent Catalyst for CO₂ Conversion. *J. Am. Chem. Soc.* **2016**, *138*, 2142–2145.
- (36) Dong, J.; Cui, P.; Shi, P.-F.; Cheng, P.; Zhao, B. Ultrastrong Alkali-Resisting Lanthanide-Zeolites Assembled by $[Ln_{60}]$ Nanocages. *J. Am. Chem. Soc.* **2015**, *137*, 15988–15991.
- (37) Lu, B.-B.; Jiang, W.; Yang, J.; Liu, Y.-Y.; Ma, J.-F. Resorcin[4]arene-Based Microporous Metal–Organic Framework as an Efficient Catalyst for CO₂ Cycloaddition with Epoxides and Highly Selective Luminescent Sensing of Cr₂O₇²⁻. *ACS Appl. Mater. Interfaces* **2017**, *9*, 39441–39449.
- (38) Spek, A. L. PLATON SQUEEZE: A Tool for the Calculation of the Disordered Solvent Contribution to the Calculated Structure Factors. *Acta Crystallogr., Sect. C: Struct. Chem.* **2015**, *71*, 9–18.
- (39) Li, X.-Y.; Ma, L.-N.; Liu, Y.; Hou, L.; Wang, Y.-Y.; Zhu, Z. Honeycomb Metal–Organic Framework with Lewis Acidic and Basic Bifunctional Sites: Selective Adsorption and CO₂ Catalytic Fixation. *ACS Appl. Mater. Interfaces* **2018**, *10*, 10965–10973.
- (40) Gao, W.-Y.; Chen, Y.; Williams, K.; Cash, L.; Perez, P. J.; Wojtas, L.; Cai, J.; Chen, Y.-S.; Ma, S. Crystal Engineering of an nbo Topology Metal–Organic Framework for Chemical Fixation of CO₂ under Ambient Conditions. *Angew. Chem., Int. Ed.* **2014**, *53*, 2615–2619.
- (41) Huang, X.; Chen, Y.; Lin, Z.; Ren, X.; Song, Y.; Xu, Z.; Dong, X.; Li, X.; Hu, C.; Wang, B. Zn-BTC MOFs with Active Metal Sites Synthesized via a Structure-Directing Approach for Highly Efficient Carbon Conversion. *Chem. Commun.* **2014**, *50*, 2624–2627.
- (42) Zhou, Z.; He, C.; Xiu, J.; Yang, L.; Duan, C. Metal–Organic Polymers Containing Discrete Single-Walled Nanotube as a Heterogeneous Catalyst for the Cycloaddition of Carbon Dioxide to Epoxides. *J. Am. Chem. Soc.* **2015**, *137*, 15066–15069.
- (43) Ng, C. K.; Toh, R. W.; Lin, T. T.; Luo, H.-K.; Hor, T. S. A.; Wu, J. Metal–Salen Molecular Cages as Efficient and Recyclable Heterogeneous Catalysts for Cycloaddition of CO₂ with Epoxides under Ambient Conditions. *Chem. Sci.* **2019**, *10*, 1549–1554.
- (44) Meng, X.; Ju, Z.; Zhang, S.; Liang, X.; von Solms, N.; Zhang, X.; Zhang, X. Efficient Transformation of CO₂ to Cyclic Carbonates Using Bifunctional Protic Ionic Liquids under Mild Conditions. *Green Chem.* **2019**, *21*, 3456–3463.

- (45) Sun, X.; Gu, J.; Yuan, Y.; Yu, C.; Li, J.; Shan, H.; Li, G.; Liu, Y. A Stable Mesoporous Zr-Based Metal Organic Framework for Highly Efficient CO₂ Conversion. *Inorg. Chem.* **2019**, *58*, 7480–7487.
- (46) Rachuri, Y.; Kurisingal, J. F.; Chitumalla, R. K.; Vuppala, S.; Gu, Y.; Jang, J.; Choe, Y.; Suresh, E.; Park, D.-W. Adenine-Based Zn(II)/Cd(II) Metal-Organic Frameworks as Efficient Heterogeneous Catalysts for Facile CO₂ Fixation into Cyclic Carbonates: A DFT-Supported Study of the Reaction Mechanism. *Inorg. Chem.* **2019**, *58*, 11389–11403.
- (47) Wei, L.-Q.; Ye, B.-H. Efficient Conversion of CO₂ via Grafting Urea Group into a [Cu₂(COO)₄]-Based Metal–Organic Framework with Hierarchical Porosity. *Inorg. Chem.* **2019**, *58*, 4385–4393.
- (48) Wang, Y.; Li, S.; Yang, Y.; Shen, X.; Liu, H.; Han, B. A fully Heterogeneous Catalyst Br-LDH for The Cycloaddition Reactions of CO₂ with Epoxides. *Chem. Commun.* **2019**, *55*, 6942–6945.
- (49) Jiang, W.; Yang, J.; Liu, Y.-Y.; Song, S.-Y.; Ma, J.-F. A Porphyrin-Based Porous rhl Metal–Organic Framework as an Efficient Catalyst for the Cycloaddition of CO₂ to Epoxides. *Chem. - Eur. J.* **2016**, *22*, 16991–16997.
- (50) Wang, X.; Gao, W.-Y.; Niu, Z.; Wojtas, L.; Perman, J. A.; Chen, Y.-S.; Li, Z.; Aguila, B.; Ma, S. A Metal–Metalloporphyrin Framework Based on an Octatopic Porphyrin Ligand for Chemical Fixation of CO₂ with Aziridines. *Chem. Commun.* **2018**, *54*, 1170–1173.
- (51) Lu, B.-B.; Yang, J.; Liu, Y.-Y.; Ma, J.-F. A Polyoxovanadate–Resorcin[4]arene-Based Porous Metal–Organic Framework as an Efficient Multifunctional Catalyst for the Cycloaddition of CO₂ with Epoxides and the Selective Oxidation of Sulfides. *Inorg. Chem.* **2017**, *56*, 11710–11720.
- (52) Wang, X.; Zhou, Y.; Guo, Z.; Chen, G.; Li, J.; Shi, Y.; Liu, Y.; Wang, J. Heterogeneous Conversion of CO₂ into Cyclic Carbonates at Ambient Pressure Catalyzed by Ionothermal-Derived Meso-Macroporous Hierarchical Poly(ionic liquid)s. *Chem. Sci.* **2015**, *6*, 6916–6924.
- (53) Zhu, J.; Usov, P. M.; Xu, W.; Celis-Salazar, P. J.; Lin, S.; Kessinger, M. C.; Landaverde-Alvarado, C.; Cai, M.; May, A. M.; Slebodnick, C.; Zhu, D.; Senanayake, S. D.; Morris, A. J. A New Class of Metal-Cyclam-Based Zirconium Metal–Organic Frameworks for CO₂ Adsorption and Chemical Fixation. *J. Am. Chem. Soc.* **2018**, *140*, 993–1003.
- (54) Ugale, B.; Dhankhar, S. S.; Nagaraja, C. M. Interpenetrated Metal–Organic Frameworks of Cobalt(II): Structural Diversity, Selective Capture, and Conversion of CO₂. *Cryst. Growth Des.* **2017**, *17*, 3295–3305.
- (55) Ugale, B.; Kumar, S.; Dhilip Kumar, T. J.; Nagaraja, C. M. Environmentally Friendly, Co-catalyst-Free Chemical Fixation of CO₂ at Mild Conditions Using Dual-Walled Nitrogen-Rich ThreeDimensional Porous Metal-Organic Frameworks. *Inorg. Chem.* **2019**, *58*, 3925–3936.
- (56) Gao, C.-Y.; Yang, Y.; Liu, J.; Sun, Z.-M. A Ni^{II}-Cluster-Based MOF as an Efficient Heterogeneous Catalyst for the Chemical Transformation of CO₂. *Dalton Trans.* **2019**, *48*, 1246–1250.
- (57) Gupta, M.; De, D.; Tomar, K.; Bharadwaj, P. K. From Zn(II)-Carboxylate to Double-Walled Zn(II)-Carboxylate Phosphate MOF: Change in the Framework Topology, Capture and Conversion of CO₂, and Catalysis of Strecker Reaction. *Inorg. Chem.* **2017**, *56*, 14605–14611.
- (58) Puthiaraj, P.; Ravi, S.; Yu, K.; Ahn, W.-S. CO₂ Adsorption and Conversion into Cyclic Carbonates over a Porous ZnBr₂-Grafted N-Heterocyclic Carbene-Based Aromatic Polymer. *Appl. Catal., B* **2019**, *251*, 195–205.
- (59) Zhou, Z.; He, C.; Yang, L.; Wang, Y. F.; Liu, T.; Duan, C. Y. Alkyne Activation by a Porous Silver Coordination Polymer for Heterogeneous Catalysis of Carbon Dioxide Cycloaddition. *ACS Catal.* **2017**, *7*, 2248–2256.
- (60) Bondarenko, G. N.; Dvurechenskaya, E. G.; Ganina, O. G.; Alonso, F.; Beletskaya, I. P. Solvent-Free Synthesis of Cyclic Carbonates from CO₂ and Epoxides Catalyzed by Reusable Alumina-Supported Zinc Dichloride. *Appl. Catal., B* **2019**, *254*, 380–390.
- (61) Yang, Y.; Gao, C.-Y.; Tian, H.-R.; Min, J.; Ai, X.; Sun, Z.-M. A Highly Stable Mn^{II} Phosphonate as a Highly Efficient Catalyst for CO₂ Fixation under Ambient Conditions. *Chem. Commun.* **2018**, *54*, 1758–1761.
- (62) Zou, R.; Li, P. Z.; Zeng, Y. F.; Liu, J.; Zhao, R.; Duan, H.; Luo, Z.; Wang, J. G.; Zou, R.; Zhao, Y. Bimetallic Metal-Organic Frameworks: Probing the Lewis Acid Site for CO₂ Conversion. *Small* **2016**, *12*, 2334–2343.